COBEM 2023 27TH INTERNATIONAL CONGRESS OF MECHANICAL ENGENEERING

ABCM Brazilian Society of Mechanical Sciences and Engineering
27th ABCM International Congress of Mechanical Engineering
December 04-08, 2023, Florianópolis-SC, Brazil

COB-2023-1983
EVALUATION OF FRICTION MATERIAL USED IN BRAKE PADS AND LININGS THROUGH DMA TESTS

Juliana Favero
Fras-le S.A. RS 122, Km 66, nº 10945 - Forqueta, RS, 95115-550, Brazil
Federal University of Rio Grande do Sul. Rua Sarmento Leite, nº 425 – Cidade Baixa – Porto Alegre, RS – Brazil
juliana.favero@fras-le.com

Roberta Motta Neves
Fras-le S.A. RS 122, Km 66, nº 10945 - Forqueta, RS, 95115-550, Brazil
roberta.neves@fras-le.com

Daniel Matté
Fras-le S.A. RS 122, Km 66, nº 10945 - Forqueta, RS, 95115-550, Brazil
University of Caxias do Sul. Rua Francisco Getúlio Vargas, 1130 - Samuel Guazzelli, Caxias do Sul - RS, 95200-000
Daniel.matte@fras-le.com

Diego Severo Antunes
Fras-le S.A. RS 122, Km 66, nº 10945 - Forqueta, RS, 95115-550, Brazil
Federal University of Rio Grande do Sul. Rua Sarmento Leite, nº 425 – Cidade Baixa – Porto Alegre, RS – Brazil
Diego.antunes@fras-le.com

Rogério Marczak
Federal University of Rio Grande do Sul. Rua Sarmento Leite, nº 425 – Cidade Baixa – Porto Alegre, RS – Brazil
00009036@ufrgs.br

Abstract. *Breaks are among the most demanding devices regarding material strength. The results of material characterization tests for such applications are generally compared with the ones obtained through numerical simulations, in order to guarantee that the stresses generated in the friction materials during the brake application do not exceed the material strength, thus ensuring its usage without failure, as cracks or displacements. Friction materials may have some level of viscoelasticity, since they use organic resins and elastomers in their formulation, even if in small amounts. Organic resins are used as a binder, joining all other components, ensuring structural integrity. Elastomers, on the other hand, are the viscoelastic components responsible for giving flexibility to the friction material, and rubbers are generally used. Thus, the main objective of the proposed work is to develop a methodology for the evaluation of friction materials using the DMA test. Test trials will be carried out with different temperatures, and these results will be used as input data for numerical simulations, using the adjustment of material elasticity modulus according to the temperature.*

Keywords: *Dynamic Mechanical Analysis, friction material, viscoelasticity, bench tests, characterization tests*

1. INTRODUCTION

Brake systems are one of the most demanding systems in the mobility segment, and their performance is a response to various components working together. Friction materials are relevant components of the brake system, once they are responsible for converting kinetic energy into thermal energy. According to Antunes et al., (2021) brake pads or brake linings are developed to have a good agreement among various characteristics, for example: friction level, durability, noise propensity and mechanical properties. Besides, friction materials during braking are exposed to different types of effort, such as compression, shear, traction and also high levels of temperature during application.

Friction materials are classified as complex composites, once their formulation is composed of various row materials (Menetrier, 2006) and (Lamb, 2008). Limpert (1999) describes the main classification of friction material components as:

- Binder: component responsible for integrating all the raw materials in the form of a rigid bulk, guaranteeing structural integrity;
- Elastomer: viscoelastic component responsible for providing flexibility to the friction material. Different grades of rubbers are generally used;

- Lubricant: component responsible for reducing the friction coefficient, making it stable and forming a thin film between the friction surfaces. Usually, graphite is used;
- Abrasive: component responsible for increasing the coefficient of friction. These raw materials have a direct impact on the useful life of the friction material and the rotor, as they are generally very aggressive;
- Reinforcement: component responsible for ensuring the mechanical resistance of the material. Usually metallic, glass or ceramic fibers are used;
- Filler: usually fillers are added to the friction material to improve processing and reduce costs. Fillers can be organic like cashew powder and rubber powder, or they can be inorganic like barite or calcium carbonate.

Menetrier (2006) remarks the selection of friction material is carried out through the evaluation of several properties of the friction materials. To evaluate these properties, chemical, physical and mechanical tests are performed.

In this work, bench characterization tests are usually carried out to verify any manufacturing inconsistency or a chemical, physical or mechanical outlier, thus it is possible to define the best proposals according to the requirements, to follow the test planning on an inertial dynamometer. The main characterization tests are: specific gravity, swelling and growth, impact strength, hardness, compressibility, damping capacity, tensile, flexural, compression and shear strength (Menetrier, 2006) (Lamb, 2008). Tensile, flexural, compression and shear strength are static tests, important to understand the limits of the friction materials (Cassu and Felisberti, 2005). DMA (Dynamic Mechanical Analysis) techniques are used to characterize the material properties under dynamic loads.

The main purpose of this study is to evaluate different friction materials using the DMA technique and correlate the results with the usual characterization and dynamometer tests. Two different friction materials were selected in order to have different levels of properties evaluated. Later, the DMA results will be used as input for numerical simulations.

2. THEORY BACKGROUND

2.1 Dynamic Mechanical Analysis

DMA is a widely used technique to characterize material properties (Lorandi et. al. 2016) (Deng et. al., 2007). This technique applies a sinusoidal cyclic force (for simplicity) to the sample, allowing us to understand the response of the material as a function of time, temperature, frequency and application load, obtaining changes in stiffness and damping as a response. In this technique, the frequency of the force application or the temperature can be varied, thus obtaining variations in the stiffness and damping of the material (Lorandi et. al., 2016) (Deng et. al., 2007).

DMA tests allow the identification of elastic and viscoelastic responses of the material. Usually, the test is performed using forced oscillations, meaning that a fixed level of stress or strain is applied on the test sample, and temperature and/or frequency are increased according to a fixed incremental value.

Three important parameters are measured using the DMA test: storage modulus, loss modulus and the loss tangent tan δ. The elastic behavior is given by the relationship of force and displacement imposed on the materials, called the storage modulus. The viscous behavior is given by the phase difference between stress and strain, also called loss modulus. This is equivalent to quantifying the delay δ between the stress and the strain responses in time. The ratio between the storage modulus and the loss modulus is called tan δ. In this context, it is important to realize that Young's modulus is obtained through destructive static tests, aiming to determine the material's failure properties, being calculated from the initial slope of the stress-strain curve. However, the storage modulus is a dynamic measure, where stress and strain are oscillatory, and its result will be a function of temperature or test frequency.

The storage modulus is the ratio between the amplitude of the stress component in phase with the strain and the strain amplitude, which can be a function of temperature or the applied frequency as mentioned before (Ferry, 1980). The definition applies to both, the Young and the shear modulus:

$$E^{'} = \frac{\sigma_0}{\varepsilon_0}\cos\delta = E^{*}\cos\delta, \tag{1}$$

$$G' = \frac{\sigma_0}{\varepsilon_0}\cos\delta = G^{*}\cos\delta, \tag{2}$$

where E' is the Young storage modulus and G' is the shear storage modulus for, σ_0 is the stress amplitude applied to the test sample, ε_0 is the strain amplitude obtained as a response to the test, and E^* and G^* are the Young and Shear complex modulus, respectively.

Ferry (1980) mentions that the loss modulus represents the energy dissipated in the form of heat in each cycle, corresponding to the viscous response of the material. It is calculated by the ratio between the amplitude of the out-of-phase stress component in relation to the strain by the strain amplitude, according to Eq. (3) and (4).

$$E'' = \frac{\sigma_0}{\varepsilon_0}\sin\delta = E^{*}\sin\delta, \tag{3}$$

$$G'' = \frac{\sigma_0}{\varepsilon_0}\sin\delta = G^{*}\sin\delta, \tag{4}$$

where E'' and G'' are the Young and shear loss modulus counterparts of E' and G'.

The ratio between the loss modulus and the storage modulus is known as the loss tangent, tan δ or damping, which is the material ability to convert mechanical energy (Lorandi et. al., 2016):

$$\frac{E^{"}}{E'} = \frac{E^* \sin\delta}{E^* \cos\delta} = \tan\delta, \tag{5}$$

It represents the phase difference between the applied stress and the resulting strain of the sample, during dynamic applications of sinusoidal load. Cassu and Felisberti (2005) mention that this parameter allows understanding the difference between the elastic and viscous components of the sample, meaning, the higher the peak of the tan δ curve, the greater the predominance of viscous behavior over the elastic one. Elastic materials have null tan δ.

3. METHODOLOGY

The methodology of the present study was divided into two stages. The first stage was the mechanical characterization, (including the DMA test) and dynamometer tests of two different friction materials. The second stage is the elaboration of a finite element model using the data retrieved from the DMA test.

Two different friction materials were selected in order to perform this investigation, material A and material B. Material A formulation uses steel wool as reinforcement and phenolic resin as binder, and it is produced through a worm press process. Material B also uses steel wool as reinforcement and phenolic resin as binder, although it has a higher volume of rubber in the mix. Material B also was produced through a worm press process although at lower temperatures than material A. Table 1 shows a summary of both formulations.

Table 1. Friction materials mix

Material	Fillers	Reinforcement	Lubricant	Binder	Elastomer	Abrasive
A	38	32	13	9	2	1
B	44	20	12	7	10	2

3.1 Mechanical characterization and dynamometer tests

As mentioned, the first stage of this study was the mechanical characterization and dynamometer test of friction materials A and B. Table 2 shows a list of the tests performed at Fras-le laboratory (FRAS-LE, 2023).

Table 2. Characterization tests.

Property	Procedure
Specific Gravity	NBR5544-2008
Gogan Hardness	NBR5520-1991
Wear rate - Fast	NBR7813-1998
Friction CoF - Chase	SAE J661-2012
DMA	-
Shear Resistance (Ultimate Shear Stress)	ISO6211-1998
Flexural Resistance (Ultimate Normal Stress)	Based on BS AU 142-1979
Impact Resistance	ASTM D256-2010 - IZOD

Specific Gravity test was performed according to the standard NBR5544-2008. In order to perform this test, the friction material needs to be separated from the metallic backing plate or the metallic shoe. After, the friction material is weighed on a scale in air and in water environment, and the result is calculated as:

$$SG = \frac{A}{A-B}\ , \tag{6}$$

where A is the measurement in the air environment and B is the measurement in the water environment.

Gogan hardness measurement was performed according to NBR5520-1991. Usually, this test is performed on three samples, and three measurements on each sample. The Gogan hardness number is interpreted as how many times 0,0064 mm of the metallic insert penetrates in the sample, and therefore higher values of Gogan hardness are found in softer materials. The test preload is 4,9 kN, the final load is 14,71 kN and the metallic insert has a diameter of 19,05 mm.

A Fast test was performed according to NBR7813-1998 and its main result is the wear rate of the friction material, although it also measures the friction coefficient. This test is similar to a disc brake application, although it is a bench

test, so the friction material sample and the disc are standardized. The dimension of the friction material sample is 12,5x12,5x3,3 mm. The test procedure is basically a drag module, so during the test, a constant friction force of 555 kPa is kept for 90 minutes and the disc angular velocity is 870 rpm. The wear rate is calculated according to (NBR7813-1991):

$$\Delta d = \frac{60000\ A\ \Delta e}{F\ V\ T}, \tag{7}$$

where Δd is the wear rate in cm^3/kWh, A is the friction area in cm^2, Δe is the wear of the sample in cm, F is the friction force in N, V is the tangential velocity measured on the effective radius in m/s and T is the total time in minutes.

Chase test was performed according to SAE J661-2012 and its main results are the normal and hot friction level of the material. The Chase test is also a bench test, where the friction sample is pressured against the internal area of the rotational drum, also in a drag module condition. The dimensions of the friction sample are 25,4x25,4x6 mm and the drum material and geometry are standardized. Figure 1 shows a summary of the test parameters.

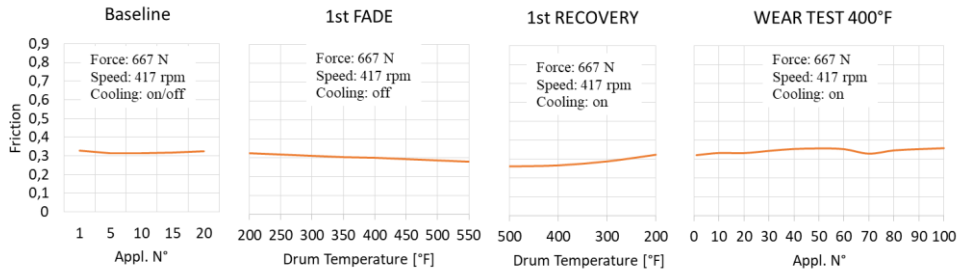

Figure 1. Chase test summary.

For this study, one DMA test of each material was performed using the three-point bending gauge. The friction material sample dimensions are 60x10x12 mm. The temperature range was from 25°C to 350°C with an increase rate of 5°C/min and the frequency was fixed at 10 Hz.

Shear resistance – Ultimate Shear Stress – test was performed according to ISO6211-1998 in a universal testing machine. This test measures the internal shear resistance of the friction material, so the sample of friction material only is placed into a device where half of it stands still, while the other half has a vertical movement, separating the sample into two pieces by a shear force. Usually, 10 samples of 20x20x10 mm are measured in order to have a good sampling.

Ultimate Normal Stress – was performed according to an internal Fras-le procedure based on the BS AU 142-1979. The test uses the three-point bending setup, and the load is applied until the sample fails. The sample dimensions are 70x25x7,4 mm and the distance between the two supports is 50 mm. The flexural resistance is calculated as:

$$FR = \frac{1{,}5\ W\ L}{B\ D^2}, \tag{8}$$

where FR is the flexural resistance, W is the rupture load, L is the distance between the supports, B is the width of the sample and D is the thickness of the sample.

Impact resistance test was performed according to the ASTM D256-2010 – IZOD test method. The sample dimensions are 64x12,7x12,7 mm, and the notch is in the V shape with an angle of 45°. During the test, the hammer hits the sample at a speed of 3,46 m/s. Usually, 10 samples are measured in order to have a good sampling.

The inertial dynamometer test performed is an internal Fras-le procedure MF82.032 aiming to compare the friction efficiency in different conditions of application. The main evaluation of this test is the friction performance stability after different temperature, speed and pressure conditions. Table 3 shows a summary of the test conditions.

Table 3. MF82.032 summary.

Section	N° Snubs	Pressure [bar]	Initial speed [km/h]	Final speed [km/h]	Initial temp. [°C]
Init. Efficiency	1	1 to 8	60	0	100
Bedding	400	3	60	20	150
Effic. after bed.	1	1 to 8	60	0	100
1st fade	30	Reach 3 m/s²	60	30	100
Effic. after fade	1	1 to 8	40/60/80/100	0	100

3.2 Finite element analysis

The finite element analysis evaluated in this study was performed using Ansys software (ANSYS, 2019). The brake application chosen was a front motorcycle disc brake, although the caliper and the disc geometries were simplified, once the authors did not have access to the real geometry.

The simulation performed was a one-way coupled thermo-mechanical analysis, according to Figure 2. The boundary conditions of the mechanical analysis are: prescribed force of 3350 N on both caliper pistons (equivalent to a pressure of 35 bar – critical brake condition for motorcycles); fixed support on the left side of the backing plate simulating the caliper housing condition; zero axial displacement for the disc (simulating the symmetric condition of both brake pads actuating on the disc surface); remote displacement applied for the disc, representing its rotation; cylindrical support for both pistons to allow axial displacement; and fixed support for the pin on the right side of the backing plate, simulating the caliper housing condition. A friction coefficient of 0,1 was used between pistons and backing plate and backing plate and caliper housing, while a friction coefficient of 0,4 was used between friction material and disc. Bonded contact was enforced between the friction material and the backing plate.

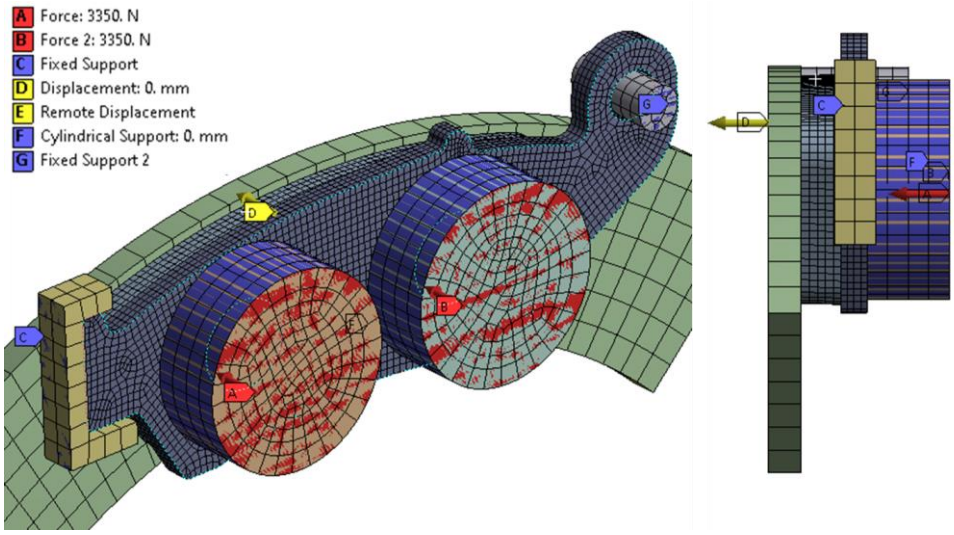

Figure 2. FEA – Boundary Conditions.

For the thermal analysis, the fixed temperature of 300°C - critical temperature for motorcycle application – was applied uniformly on the disc brake. A constant convection coefficient of 200 W/m² °C was applied for the friction material, in order to evaluate its temperature.

The DMA result of storage modulus and loss modulus x temperature of the friction materials was applied as the input of Young's Modulus data, according to Table 4. For material A, eight points are enough to discretize the curve, although, for material B, ten points show a better discretization. For the packing plate, made of steel grade ASTM A36, the mechanical properties with temperature are shown in Table 5 (MILKE ET AL, 2014). These results were used as three bilinear models in Ansys software, at temperatures of 25°C, 135°C and 245°C.

Table 4. DMA results used as input to Young's modulus in the FEA.

Material A				**Material B**			
Temp [°C]	**E' [MPa]**	**E'' [MPa]**	**E* [MPa]**	**Temp [°C]**	**E' [MPa]**	**E'' [MPa]**	**E* [MPa]**
22	5645	479	5665	27	6662	326	6670
51	5518	443	5535	50	6435	353	6445
101	5280	431	5298	100	3127	437	3157
151	5286	421	5303	125	1968	290	1990
201	5212	415	5228	151	1460	187	1472
251	4178	596	4220	201	1038	140	1047
301	4066	421	4087	225	869	148	882
349	4201	290	4211	251	966	140	976
				300	1098	141	1107
				348	245	27	247

Table 5. ASTM A36 mechanical properties with temperature – Bilinear Model.

Temp [°C]	Young's Modulus [GPa]	Tangent Modulus [GPa]	Yield Strength [MPa]
25	200	1,078	290
135	190,5	1,177	260
245	181	1,128	230

4. RESULTS AND DISCUSSION

4.1 Mechanical characterization and dynamometer tests

The results of the mechanical characterization are comparatively shown in Figures 3 to 6 for both materials studied. The error bar was set to be the minimum and the maximum values found in the tests. Figures 7 and 8 show the dynamometer results.

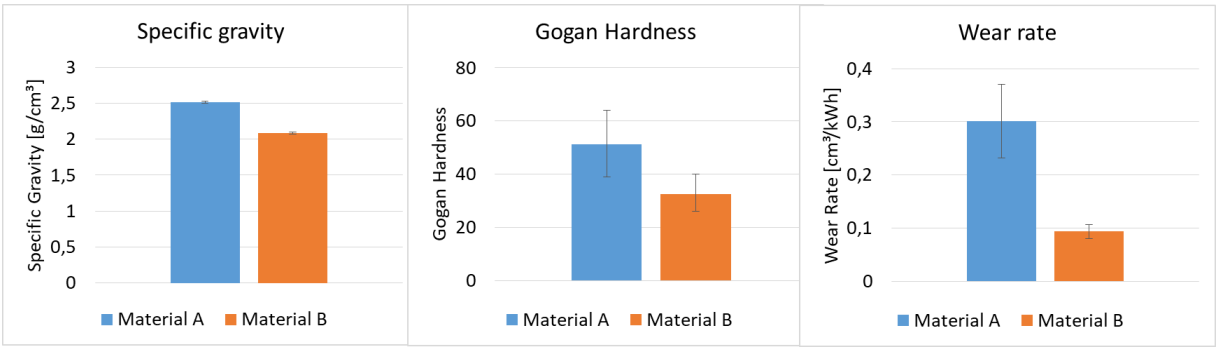

Figure 3. Characterization results – Specific gravity, Gogan hardness and Fast wear test.

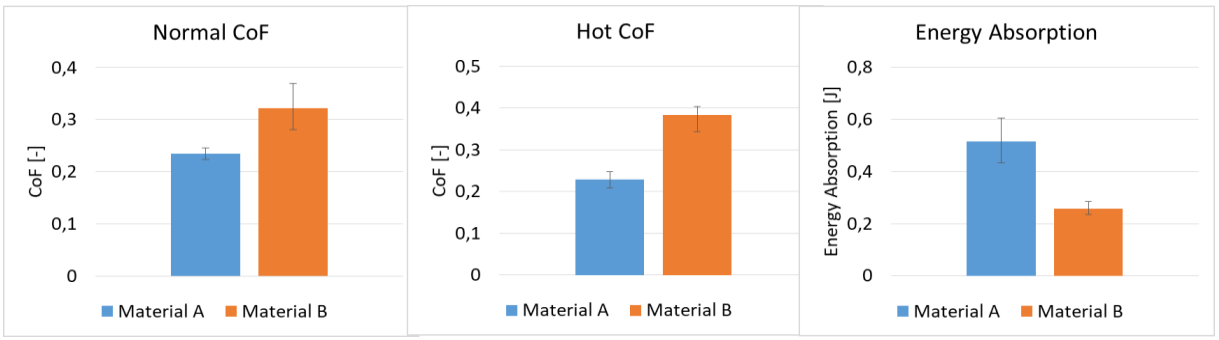

Figure 4. Characterization results – Chase normal and hot CoF and Energy Absorption of the Impact test.

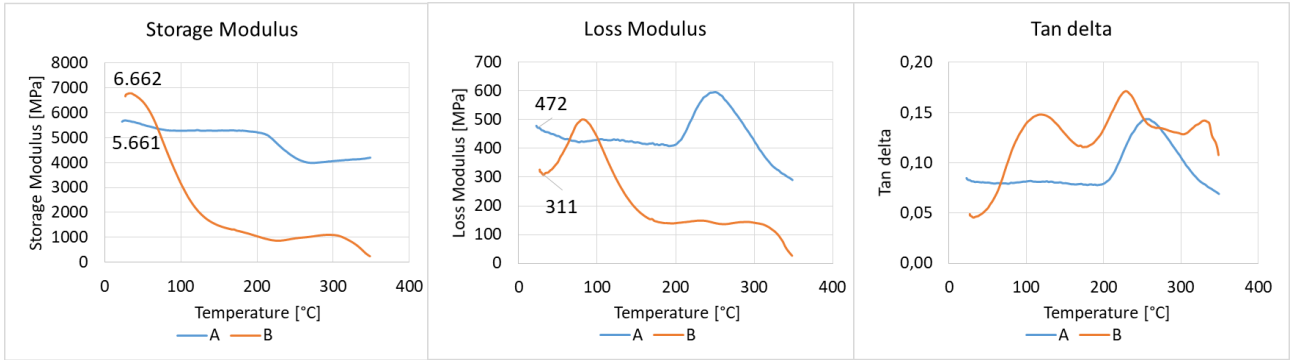

Figure 5. Characterization results - DMA.

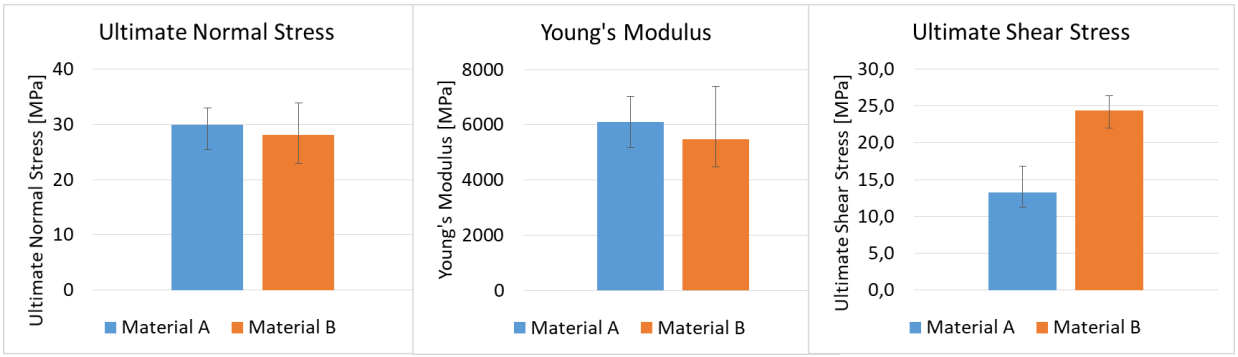

Figure 6. Characterization results – Ultimate Normal Stress and Ultimate Shear Stress.

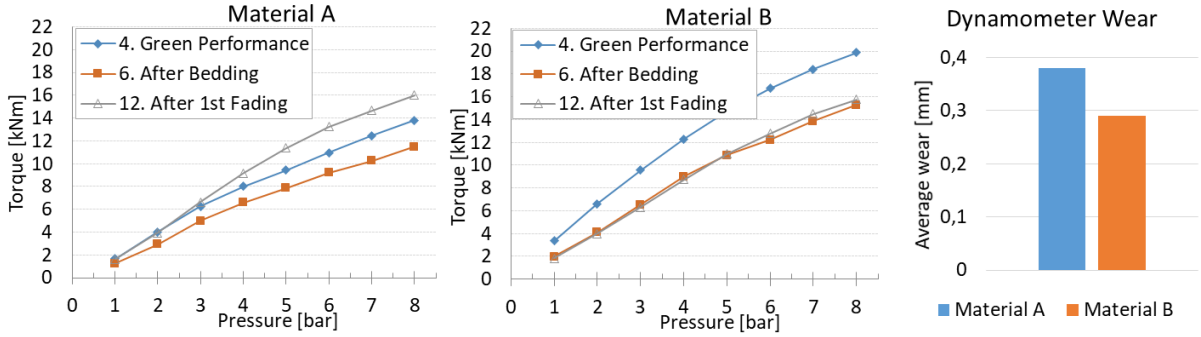

Figure 7. Dynamometer results – Efficiency and wear.

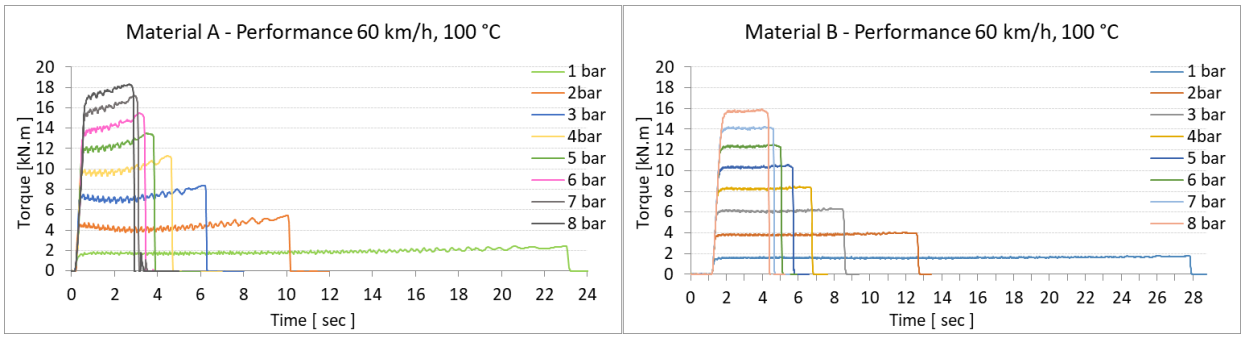

Figure 8. Dynamometer results – Torque x time.

Comparing and analyzing some of the characterization results, it is possible to correlate some of the characteristics between the tests.

Material A shows a lower normal and hot friction level than material B, according to Figure 4. Therefore material A shows a higher wear rate in the Fast test, according to Figure 3. This behavior is usual, once the Fast test is controlled by a fixed friction force, thus in order to reach that force, material A will be under a higher normal force than material B, and as a consequence, it will show a higher wear rate.

Material A shows a higher Gogan hardness (NBR 5520-1991) than material B, according to Figure 3, meaning that material A is softer than material B. This result also correlates with the wear rate, meaning that softer materials will have a higher contact area with the rotor, causing higher wear. Gogan hardness result also can be correlated to the energy absorption of the impact resistance test - Figure 4 - where material A shows a significantly higher energy absorption than material B.

It is also possible to correlate Young's modulus obtained through the flexural resistance test (Figure 6) with the Storage and the Loss modulus obtained through the DMA test (Figure 5). Young's modulus is the sum of the vector components of the Storage and the Loss modulus, thus to correlate both tests it is necessary to evaluate the equation:

$$E^* = \sqrt{(E')^2 + (E'')^2}, \tag{9}$$

Calculating Eq. (9) for materials A and B results in 5680 MPa and 6669 MPa, respectively. Evaluating the results of Young's Modulus in Figure 6, it is possible to see that both results calculated previously are contemplated by the error bar.

Evaluating the dyno tests, it is possible to correlate some of the efficiency test results with the characterization results. Figure 7 shows the torque efficiency for both materials and material A shows lower torque results than material B, correlating with Figure 4 Chase normal and hot CoF results. From Figure 7 it is also possible to notice that both friction materials have different performance characteristics. Material A shows an increase in performance after the first fade while material B shows a decrease in performance after the bedding section and the performance level is stable after the first fade.

Analyzing wear results from the dyno test in Figure 7, it is also correlated with the wear of both materials in the Fast test – Figure 3 – where material A has higher wear than material B. It is clear that the magnitudes can not be correlated, once the Fast is a bench test with only one friction force condition, while the dyno test uses the entire brake device and it simulates various brake conditions. However, the Fast bench test can be used to narrow down the different versions of formulation before dyno testing.

Figure 8 shows the torque × time curves for both materials in different brake pressure and temperature conditions. For material A, it is possible to notice that for all conditions the torque oscillation is higher than material B. This result can be correlated with tan δ results from Figure 5, which is the material damping. In Figure 5, material A shows lower results of tan δ for 100°C and 200°C than material B, meaning it has a lower capacity of vibration absorption and consequently higher torque oscillations. Hwang, et al (2010) find the same correlation in their study, where materials with higher tan δ results show less friction coefficient oscillation during testing.

4.2 Finite element analysis

The FEA was performed using a mesh of 18763 quadratic elements, resulting in 278631 degrees of freedom. The elements used were Hex20 and Wed15, element type SOLID183 with reduced integration. The simulation time was 296 minutes for each material. No mesh convergence analysis was performed for this study, as the case is a well-known one, incorporating the knowledge of previous similar cases in the industry.

Figure 9 shows the results of the thermal analysis. Since materials have the same convection coefficient, the results are the same for both.

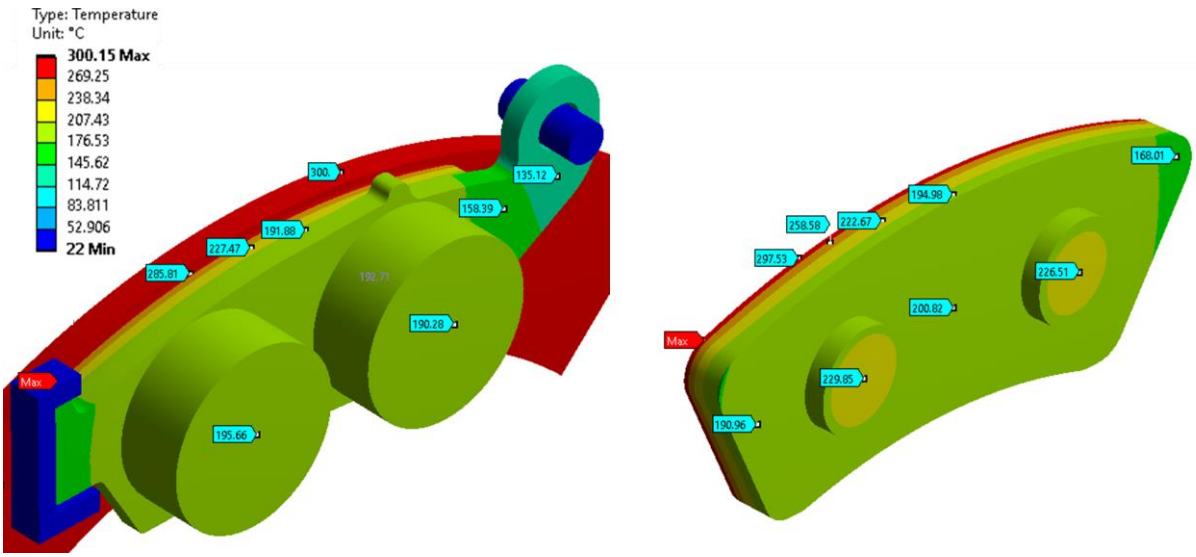

Figure 9. FEA results – Thermal analysis.

It is possible to notice in Figure 9, that using a critical temperature of 300°C in the disc, the friction material will present temperatures from almost 300°C very near to the disc surface, and temperatures around 200°C close to the backing plate. It is also noticeable that the left side of the backing plate reaches higher temperatures than the right side. This is due to the higher dissipation area on the right side.

Figure 10 shows the mechanical response of the main parts under the loading considered.

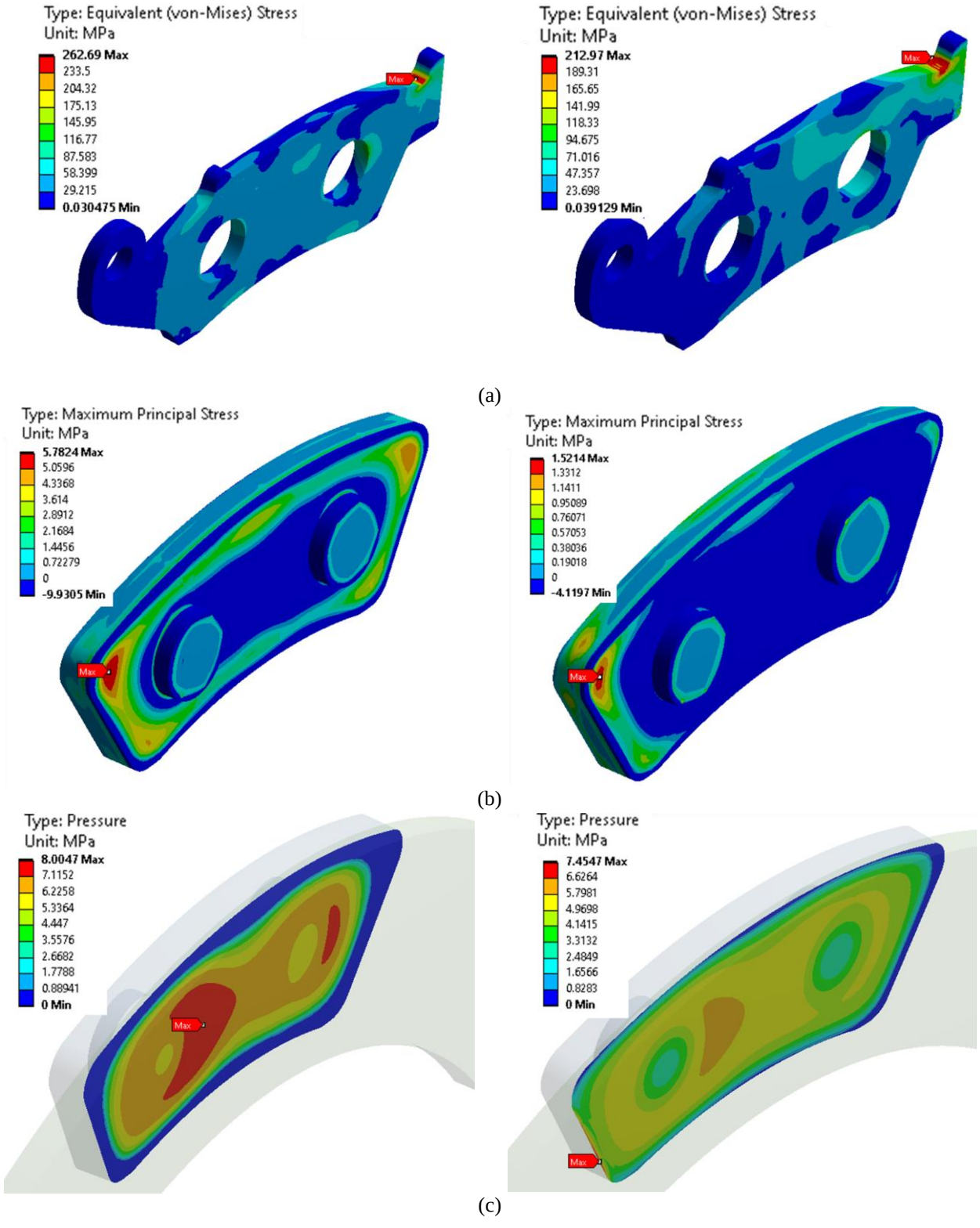

Figure 10. FEA results materiaisl A and B respectively – (a) Von Misses Stress on the backing plate; (b) Maximum principal stress on the friction material; (c) Contact pressure between friction material and disc.

The results of the equivalent Von Misses stress on the backing plate – Figure 10(a) – are very similar for both materials, although material A, which has a higher and more stable Young's Modulus, happens to show higher values of stress. This effect can be correlated with less elastic strain for friction material A – 0,48% for material A and 1,35% for material B. The results of Maximum Principal Stress – Figure 10(b) – on the friction materials A and B show the highest values of stress occurring at the same spot, nearest to the highest stress of the baking plate, concluding this is a critical area for friction material fractures. Material A shows significantly higher stress, also due to higher values of Young's

modulus, generating less strain and therefore higher values of stress. The Maximum Principal Stress is usually compared to the ultimate shear strength of the material, as this is the lowest strength among compression, flexural and shear. The average of ultimate shear resistance is 13 MPa and 24 MPa, for materials A and B, respectively, according to Figure 6. This means that both materials have higher chances to be applied for this brake with no failures. At last, the contact pressure between friction material and disc – Figure 10(c) – also shows the same behavior for both materials, although material B has a more uniform pressure distribution, also due to the lower values of Young's modulus.

5. CONCLUSIONS

This study presented an analysis methodology that allows the correlation of some DMA results with other characterization results and also dynamometer tests for two materials typically used in break devices. For example, the Young's Modulus calculated through the ultimate normal stress was correlated with the Young's modulus calculated using the DMA results. It was also possible to correlate the loss modulus from the DMA results with the friction coefficient oscillations during the dynamometer test.

The FEA results showed that both materials can be applied for motorcycle brake pads, once the severe temperature and pressure conditions are up to 300°C and 35 bar, respectively. This simulation process should be applied to other brake applications that are more critical, for example, heavy-duty vehicles, in order to validate the materials to be used commercially. For each application, it is important to understand the critical conditions of pressure and temperature, and if necessary, repeat the DMA test at higher temperatures, to use its results as data for the simulation, following the methodology proposed herein.

6. REFERENCES

ABNT. NBR 5544-1998: Guarnições da embreagem e do freio - Determinação da densidade relativa. RJ, 1998. 2 p.

ABNT. NBR 5520-1991: Guarnições de freio - Determinação da dureza "Gogan" de materiais de fricção. RJ, 1991. 4 p.

ABNT. NBR 7813-1998: Guarnições da embreagem e do freio - Material de fricção do tipo orgânico - Verificação das características de fricção e desgaste - Ensaio FAST. Rio de Janeiro, 1998. 10 p.

ANSYS Help Documentations, version R2, 2019.

Antunes, Diego Severo; Brezolin, André; Favero, Juliana; Wille, Norton Hernandez; Bastos, Saulo Renê Casarin; Luza, Thaysa. Influence analysis of brake linings roughness on static friction coefficient between brake linings and shoes. SAE Technical Paper Series, Caxias do Sul, v. 36, n. 428, p. 1-7, 10 fev. 2022. SAE International.

ASTM. ASTM D256-2010: Standard Test Method for Determining the Izod Pendulum Impact Resistance of Plastics. West Conshohocken, 2010. 20 p.

BS AU. BS AU 142-1979: Methods of Test for Brake Linings Materials. London, 1979.

Cassu, Silvana N.; Felisberti, Maria I. Comportamento dinâmico-mecânico e relaxações em polímeros e blendas poliméricas. Química Nova, [S.L.], v. 28, n. 2, p. 255-263, 2005. FapUNIFESP (SciELO).

Deng, Shiqiang; Hou, Meng; Ye, Lin. Temperature-dependent elastic moduli of epoxies measured by DMA and their correlations to mechanical testing data. Polymer Testing, [S.L.], v. 26, n. 6, p. 803-813, set. 2007. Elsevier BV.

Ferry, John D. Viscoelastic properties of polymers. John Willey and Sons, 1980.

Fras-le (Brasil). Fras-le. Disponível em: https://www.fras-le.com/pt/. Acesso em: 21 jun. 2023.

Hwang, H.J.; Jung, S.L.; Cho, K.H.; Kim, Y.J.; Jang, H.. Tribological performance of brake friction materials containing carbon nanotubes. Wear, [S.L.], v. 268, n. 3-4, p. 519-525, fev. 2010. Elsevier BV.

Lamb, Ricardo G. Estudo do comportamento de desgaste de material de atrito em função de variáveis de aplicação. 2008. 141f. Master's thesis, Graduate Program in Materials Engineering, University of Caxias do Sul, Caxias do Sul, Brasil.

Limpert, Rudolf. Brake design and safety. EUA. Society of Automotive Engineers International, 1999.

Lorandi, Natalia P.; Cioffi, Maria Odila H.; Ornaghi, Junior, H. Análise Dinâmico-Mecânica de Materiais Compósitos Poliméricos. Scientia Cum Industria, v. 4, n. 1, p. 48, 2 abr. 2016. University of Caxias do Sul, Caxias do Sul, Brasil.

Menetrier, Ademir R. Estudo de variáveis de composição e processo para controle da compressibilidade. 2006. 106 f. Master's thesis, Graduate Program in Materials Engineering, University of Caxias do Sul, Caxias do Sul, Brasil.

MF82.032: Ensaio padrão de eficiência em dinamômetro para avaliação de lonas comerciais. Caxias do Sul, 2010.

Milke, James; Kodur, Venkatesh; Marrion, Christopher. An Overview of Fire Protection in Buildings. Research Gate, Michigan, 03 jun. 2014.

SAE. SAE J661-2012: Brake Lining Quality Test Procedure. 5 ed. Warrendale, 2012. 7 p.

7. RESPONSIBILITY NOTICE

The authors are the only responsible for the printed material included in this paper.